Cancer Chemother Pharmacol (2003) 52: 291–302
DOI 10.1007/s00280-003-0672-2

ORIGINAL ARTICLE

**Sonali M. Smith · Susan M. Ludeman
Lynette R. Wilson · James B. Springer
Mihir C. Gandhi · M. Eileen Dolan**

Selective enhancement of ifosfamide-induced toxicity in Chinese hamster ovary cells

Received: 30 December 2002 / Accepted: 14 May 2003 / Published online: 4 July 2003

Abstract *Purpose*: O^6-Benzylguanine (BG) is a unique purine analog that has been shown to influence nitrogen mustard activity and increase cytotoxicity. Ifosfamide is a nitrogen mustard with growing clinical applications; effective modulation may lead to improved efficacy. We thus undertook a preliminary investigation of BG's effects on ifosfamide and ifosfamide derivatives in vitro. *Experimental design*: BG's effect on ifosfamide toxicity was studied in CHO cells transfected with O^6-alkylguanine-DNA alkyltransferase (AGT) (CHO^{wtAGT}) or control plasmid pcDNA3 (CHO^{pcDNA}) using five ifosfamide derivatives and two control compounds: 4-hydroperoxyifosfamide (4HI), isophosphoramide mustard (IPM), phenylketoifosfamide (PKIF), 4-hydroperoxydidechloroifosfamide (4HDI), chloroacetaldehyde (CAA), didechloroisophosphoramide mustard (d-IPM), didechlorophenylketoifosfamide (d-PKIF). To further explore the mechanism of interaction, BG's effect on apoptosis (annexin V-FITC) and cell cycle distribution in cells exposed to ifosfamide was also analyzed. *Results*: BG substantially enhanced cytotoxicity induced only by agents that produce IPM (4HI, IPM, PKIF) in both CHO^{wtAGT} and CHO^{pcDNA} cell lines. BG did not modulate 4HDI or CAA cytotoxicity. The addition of BG to IPM in CHO cells increased the percentage of apoptotic cells from 5.5% to 28.9% at 72 h after treatment. Cell cycle analysis showed that BG exposure was associated with G_1 arrest. At 16 h following treatment with IPM, PKIF, or phosphoramide mustard (PM), BG increased the percentage of cells in G_1 from 16–20% to 29–64%. *Conclusions*: BG's ability to increase 4HI-, IPM-, and PKIF-mediated cytotoxicity in cells devoid of AGT activity suggests a novel AGT-independent mode of action that is associated with increased apoptosis and may involve G_1 arrest. BG selectively enhanced IPM toxicity without enhancement of acrolein and CAA toxicity. The data strongly support further investigation into combinations of BG and nitrogen mustards.

Keywords Ifosfamide · O^6-Benzylguanine · Cell cycle · Apoptosis · Interstrand crosslink · CHO cells

Abbreviations *4HC* 4-Hydroperoxycyclophosphamide *4HDI* 4-Hydroperoxydidechloroifosfamide · *4HI* 4-Hydroperoxyifosfamide · *AGT* O^6-Alkylguanine-DNA alkyltransferase · *AIF* Aldoifosfamide · *AP* Aldophosphamide · *BG* O^6-Benzylguanine · *CAA* Chloroacetaldehyde · *CDK* Cyclin-dependent kinase · *CHO* Chinese hamster ovary · *d-IPM* Didechloroisophosphoramide mustard · *d-PKIF* Didechlorophenylketoifosfamide · *4-HO-CP* 4-Hydroxycyclophosphamide · *4-HO-IF* 4-Hydroxyifosfamide · *ICL* Interstrand crosslink · *IPM* Isophosphoramide mustard · *PI* Propidium iodide · *PKIF* Phenylketoifosfamide · *PM* Phosphoramide mustard · *THF* Tetrahydrofuran

This work was supported in part by NIH grants CA57725 (M.E.D.), CA81485 (M.E.D.) and CA16783 (S.M.L.). S.M.S. is supported by NIH Training Grant T32-CA09566.

S. M. Smith · L. R. Wilson · M. E. Dolan (✉)
Department of Medicine, University of Chicago, Chicago, IL 60637, USA
E-mail: edolan@medicine.bsd.uchicago.edu
Tel.: +1-773-7024441
Fax: +1-773-7020963

M. E. Dolan
Committee on Clinical Pharmacology, University of Chicago, Chicago, IL 60637, USA

M. E. Dolan
Cancer Research Center, University of Chicago, Chicago, IL 60637, USA

S. M. Ludeman · J. B. Springer · M. C. Gandhi
Department of Medicine, Duke University Medical Center, Durham, NC 27710, USA

S. M. Ludeman · J. B. Springer · M. C. Gandhi
Duke Comprehensive Cancer Center, Duke University Medical Center, Durham, NC 27710, USA

M. E. Dolan
University of Chicago, 5841 S. Maryland Ave., Box MC2115 Chicago, IL 60637, USA

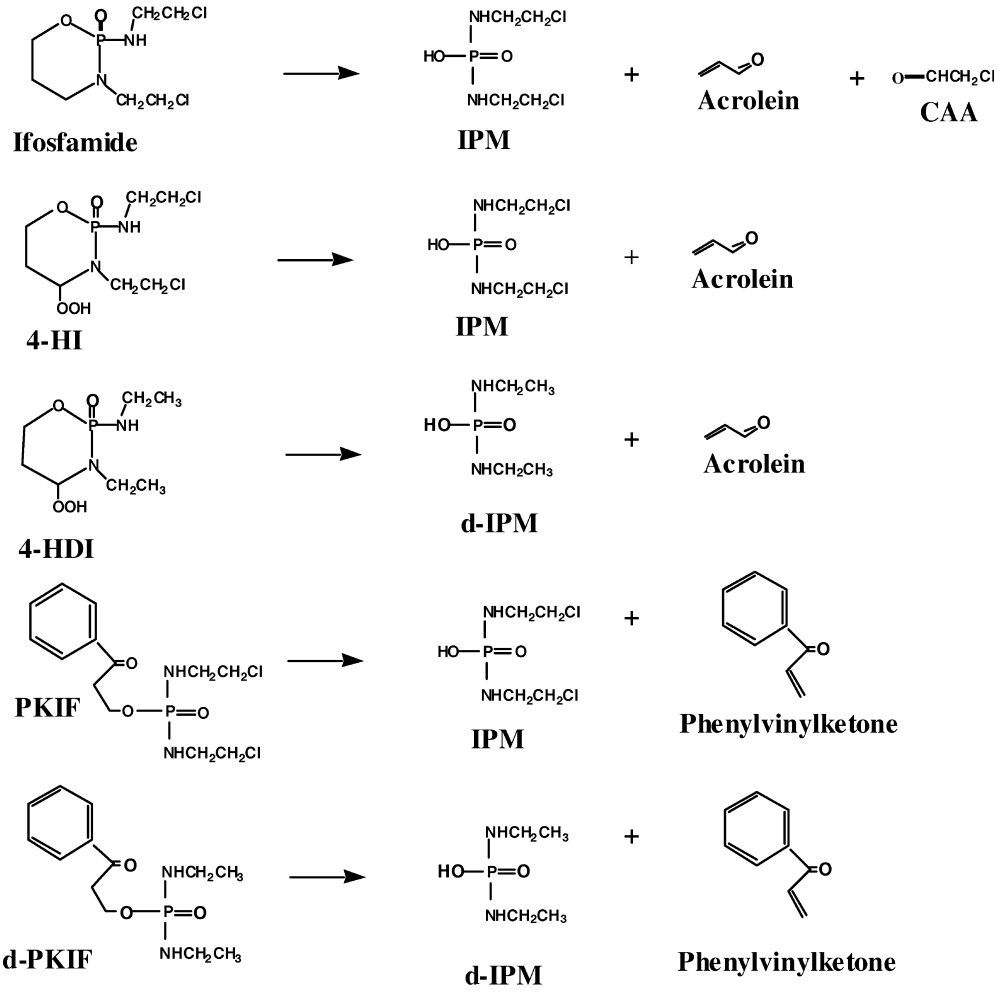

Fig. 1 Metabolic conversion of ifosfamide and spontaneous (nonenzymatic) conversions of 4HI, 4HDI, PKIF, and d-PKIF to metabolites. Ifosfamide and 4HI produce acrolein and IPM via the intermediates 4-HO-IF and AIF. Similarly, 4HDI produces acrolein and d-IPM via intermediary didechloro analogs of 4-HO-IF and AIF. PKIF and d-PKIF fragment directly to IPM/phenylvinylketone and d-IPM/phenylvinylketone, respectively

Introduction

Despite the growing number of available agents designed to arrest cancer growth, alkylating agents remain an important mainstay of cancer therapeutics. However, effective modulation of existing agents is necessary both to improve efficacy and to attenuate toxicity. Of the clinically useful alkylating agents, ifosfamide is an important component of chemotherapy regimens for a variety of solid and hematologic malignancies [1, 2, 3, 4, 5], and is thus an important target for manipulation. Major clinical toxicities include urotoxicity, nephrotoxicity, neurotoxicity, and, to a lesser extent, a risk of secondary leukemias [6]. Although urotoxicity is largely abrogated with the use of intravenous fluids and mesna [7], other side effects such as neurotoxicity and nephrotoxicity remain important limitations of therapy. Furthermore, intrinsic and acquired tumor resistance remain obstacles to improved clinical outcome. Thus, modulation of the effects of ifosfamide on malignant and normal cells is an area in need of further development.

Ifosfamide is a member of the oxazaphosphorine family of nitrogen mustards [8]. Similar to its more commonly used isomer, cyclophosphamide, ifosfamide is a prodrug which undergoes hepatic activation at the C-4 position by the P450 system to produce a therapeutically beneficial alkylating species [8]. Competing with reaction at the C-4 site is oxidation of a side chain leading to production of undesired toxic substances [9]. The key structural difference between cyclophosphamide and ifosfamide lies in the altered position of a single chloroethyl moiety from the N-2 position on cyclophosphamide to the N-3 position on ifosfamide [8]. This seemingly small change in structure significantly impacts the distribution of C-4 and side chain oxidations in ifosfamide (approximately 50:50) relative to that in cyclophosphamide (approximately 90:10). The desirable oxidation at the C-4 position in ifosfamide gives 4-hydroxyifosfamide (4-HO-IF). This metabolite interconverts with aldoifosfamide (AIF). The fragmentation of AIF provides isophosphoramide mustard (IPM) and acrolein (Fig. 1) [7]. IPM is credited with exerting most of the therapeutic effects of ifosfamide whereas acrolein is responsible for ifosfamide's severe urotoxicity [10, 11].

Until the introduction of mesna, ifosfamide-induced hemorrhagic cystitis was a severe limitation. Currently, judicious use of fluids with mesna has significantly

decreased but not eliminated the incidence of hemorrhagic cystitis. P450 oxidation of a side chain in ifosfamide occurs predominantly at the N-3 position, resulting in *N*-dechloroethylation and formation of the toxic byproduct, chloroacetaldehyde (CAA), that is implicated in ifosfamide-mediated neurotoxicity [8, 9, 12]. Although methylene blue is frequently administered to treat ifosfamide-induced mental status changes, multiple doses are required and reversal of neurotoxicity may not occur for several days [13]. Thus, manipulations intended to increase ifosfamide efficacy can be limited by concomitant increases in undesirable byproducts.

At a molecular level, ifosfamide induces toxicity via DNA alkylation and interstrand crosslink (ICL) formation primarily through its major alkylating metabolite, IPM. Specifically, IPM is a bifunctional alkylating agent producing a seven-atom ICL [14]. Although nitrogen mustards produce monofunctional guanine-N7 adducts as well as interstrand N7-N7 crosslinks involving the two guanines in GNC-GNC ($5' \rightarrow 3'/5' \rightarrow 3'$) sequences [15, 16, 17], recent evidence demonstrates that the crucial damage inflicted by nitrogen mustards is the ICL itself [18]. The contributory role of intrastrand crosslinks is unknown, but may also be important. Repair of DNA crosslinks is not fully understood; however, there is evidence that repair of ICLs introduced by nitrogen mustards is different in cycling versus noncycling cells [19]. The impact of differential repair of DNA crosslinks is that agents altering the cell cycle can be exploited to maximize the desired efficacy of nitrogen mustards while minimizing unwanted toxicities [20].

BG is a potent inactivator of the DNA repair protein AGT, resulting in an increase in the amount of damage at the O^6 position of guanine in DNA by alkylnitrosoureas and alkyltriazenes [21, 22]. Previous work in our laboratory has demonstrated that BG effectively enhances both the toxicity and mutagenicity of these alkylating agents in cell lines expressing AGT [23]. BG has recently been shown to increase the cytotoxicity of 4HC, an activated form of cyclophosphamide [23]. The mechanism of this enhancement has not been elucidated. We extended our studies to determine the cellular consequences of BG on ifosfamide metabolites responsible for antitumor activity (IPM) as well as those ifosfamide metabolites associated with unwanted side effects (acrolein, CAA).

Materials and methods

Materials

BG was generously provided by Dr. Robert C. Moschel (NCI-FCRDC, Frederick, Md.). 4HI and PKIF were synthesized as described previously [24, 25, 26]. Phosphoramide mustard (PM), as the cyclohexyl ammonium salt, and IPM were gifts from the Drug Synthesis and Chemistry Branch, Division of Cancer Treatment, National Cancer Institute. CAA was obtained from Sigma Chemical Co. (St. Louis, Mo.).

Synthesis of 4HDI

Under an atmosphere of N_2, a solution of 3-buten-1-ol (7.2 mmol, 0.62 ml) and triethylamine (7.9 mmol, 1.10 ml) in THF (dried/distilled, 7.5 ml) was added dropwise to a solution of freshly distilled phosphorus oxychloride (7.5 mmol, 0.70 ml) in THF (15 ml) at 5°C (water/ice bath). After complete addition, the reaction mixture was stirred at 5°C for 45 min. A solution of ethylamine (36 mmol; 18 ml of a 2.0 *M* solution in THF) was added quickly and then the ice bath was removed and the mixture was stirred at room temperature for 48 h. The reaction mixture was diluted with water (100 ml) and extracted with ethyl acetate (4×50 ml) and then with methylene chloride (4×30 ml). The combined organic layers were dried ($MgSO_4$), filtered and concentrated on a rotary evaporator. The resultant oil was flash chromatographed on silica gel (230–400 mesh, 1.9×20 cm column) using ethyl acetate to remove faster eluting impurities and then 5% ethanol in ethyl acetate to elute product (R_f 0.31 in 10% ethanol/ethyl acetate). The product 3-butenyl *N*,*N*′-diethylphosphorodiamidate [$CH_2=CHCH_2CH_2O$-$P(O)(NHCH_2CH_3)_2$] was obtained as an oil in 93% yield (1.39 g, 6.7 mmol). ^{1}H NMR ($CDCl_3$) δ 5.89–5.74 (m, 1H, vinylic), 5.17–5.02 (m, 2H, vinylic), 4.00 (apparent q, $J=7$ Hz, 2H, CH_2O), 3.03–2.85 (m, 4H, two CH_2CH_3), 2.57–2.34 (m, 4H, two NH and CH_2CH_2O), and 1.14 (t, $^3J_{HH}=7$ Hz, 6H, two CH_3). ^{13}C NMR ($CDCl_3$) δ 134.2 ($CH=CH_2$), 117.2 ($CH=CH_2$), 64.09 (d, $^2J_{CP}=5$ Hz, CH_2O), 36.14 (NCH_2), 35.19 (d, $^3J_{CP}=7$ Hz, CH_2CH_2O), and 17.76 (d, $^3J_{CP}=7$ Hz, CH_3).

Ozone was bubbled through a cold (0°C) solution of 3-butenyl *N*,*N*′-diethylphosphorodiamidate (3.9 mmol, 0.8 g) in acetone/water (2:1, 21 ml) for 30 min. Acetone was added to replace any that had evaporated and the reaction solution was transferred to a round bottom flask. Aqueous H_2O_2 (0.8 ml of a fresh 30% solution) was added and the flask was then stoppered and kept overnight at room temperature. Acetone was removed at ambient temperature on a rotary evaporator and the residual aqueous mixture was extracted with CH_2Cl_2 (6×20 ml). The combined organic layers were dried ($MgSO_4$), filtered, and concentrated at ambient temperature on a rotary evaporator. The resultant solid was mixed with ether (2–3 ml) and the mixture was stored at −20°C for 4 days (although overnight would have been sufficient). The supernatant was removed by pipette and the crystals were washed four times with ether (2–3 ml). After drying under vacuum, 4HDI was obtained as a white solid (0.31 g, 1.5 mmol, 38% yield). In the proton NMR spectrum, the value of the $^3J_{HP}$ that was measured for the C_4-H was consistent with an assignment of *cis* stereochemistry (a predominant 1,3-diaxial relationship between the OOH and P=O groups) [27]. ^{1}H NMR ($CDCl_3$) δ 10.67–10.16 (brs, 1H, OOH), 5.09–4.37 (m, 2H, C_4-H and one C_6-H), 4.20–4.03 (m, 1H, one C_6-H), 3.34–3.16 (m, 2H, NCH_2), 3.01–2.77 (m, 2H, NCH_2), 2.58–2.45 (brm, 1H, NH), 2.36–2.25 (m, 1H, one C_5-H), 2.09–1.94 (m, 1H, one C_5-H), and 1.14 (dt, $^3J_{HH}=7$ Hz, $^4J_{HP}=7$ Hz, 6H, two CH_3). (*Note:* The $CDCl_3$ was washed with a solution of $NaHCO_3$ in D_2O and dried with $MgSO_4$ prior to use as the NMR solvent. Acid contamination of $CDCl_3$ can cause decomposition of hydroperoxides such as 4HDI.)

Synthesis of d-PKIF

Under an atmosphere of N_2, a solution of 3-phenyl-3-buten-1-ol [26] (20 mmol, 2.98 g) in CH_2Cl_2 (dried/distilled, 20 ml) was added dropwise to a solution of phosphorus oxychloride (20 mmol, 1.86 ml) and triethylamine (20 mmol, 2.78 ml) in CH_2Cl_2 (20 ml) at −10°C (ice/salt bath). After complete addition, the reaction mixture was stirred at −10°C for 3 h. A solution of ethylamine (40 mmol; 20 ml of a 2.0 *M* solution in THF) was added dropwise to the reaction mixture followed by the dropwise addition of triethylamine (40 mmol, 5.6 ml). The reaction mixture was then stirred at room temperature for 3 days. The mixture was concentrated on a rotary evaporator and the resultant oil was flash chromatographed on silica gel (230–400 mesh, 5.5×18 cm column) using 1.25% ethanol in ethyl acetate (approximately 1000 ml) to

remove faster eluting impurities and then 2.5% ethanol in ethyl acetate to elute product (R_f 0.25 in 5% ethanol/ethyl acetate). The product, 3-phenyl-3-butenyl *N*,*N*′-diethylphosphorodiamidate [$CH_2=C(C_6H_5)CH_2CH_2OP(O)(NHCH_2CH_3)_2$] was obtained as an oil in 26% yield (1.46 g, 5.2 mmol). ^{1}H NMR ($CDCl_3$) δ 7.43–7.24 (m, 5H, aromatic), 5.36 (apparent s, 1H, vinylic), 5.14 (d, ^2J = ~1 Hz, 1H, vinylic), 4.04 (apparent q, J = 7 Hz, 2H, CH_2O), 2.98–2.80 (m, 6H, allylic and two NCH_2), 2.37–2.21 (br m, 2H, two NH), and 1.08 (apparent t, J = 7 Hz, 6H, two CH_3). ^{13}C NMR ($CDCl_3$) δ 144.4 ($C=CH_2$), 140.6, 128.5, 127.7, and 126.1 (aromatic), 114.6 ($C=CH_2$), 63.69 (d, $^2J_{CP}$ = 5 Hz, CH_2O), 36.70 (d, $^3J_{CP}$ = 7 Hz, CH_2CH_2O), 36.17 (NCH_2), and 17.80 (d, $^3J_{CP}$ = 7 Hz, CH_3). ^{31}P NMR ($CDCl_3$) δ 15.3 (referenced externally to a capillary insert of 25% H_3PO_4 in $CDCl_3$).

Ozone was bubbled through a cold (0°C) solution of 3-phenyl-3-butenyl *N*,*N*′-diethylphosphorodiamidate (2.2 mmol, 0.62 g) in acetone/water (2:1, 21 ml) for 30 min. Acetone was added to replace any that had evaporated and the reaction solution was transferred to a round bottom flask. Aqueous H_2O_2 (0.8 ml of a fresh 30% solution) was added and the flask was then stoppered and kept overnight at room temperature. Acetone was removed at ambient temperature on a rotary evaporator and the residual aqueous mixture was extracted with CH_2Cl_2 (6×25 ml). The combined organic layers were dried (Na_2SO_4), filtered, and concentrated at ambient temperature on a rotary evaporator. The resultant oil was flash chromatographed on silica gel (230–400 mesh, 4×14 cm column) using ethyl acetate (approximately 400 ml) to remove faster eluting impurities and 10% ethanol in ethyl acetate to elute product (R_f 0.28 in 10% ethanol/ethyl acetate). The product d-PKIF was obtained as a thick oil that solidified to a waxy solid upon standing at −20°C (0.29 g, 1.0 mmol, 45% yield). Analysis calculated for $C_{13}H_{21}N_2O_3P$, theory (found): C, 54.91 (54.85); H, 7.46 (7.46); N, 9.85 (9.69). ^{1}H NMR ($CDCl_3$) δ 8.01–7.43 (m, 5H, aromatic), 4.46–4.33 (m, 2H, CH_2O), 3.35 (t, $^3J_{HH}$ = 7 Hz, $CH_2C=O$), 3.05–2.86 (br m, 4H, two NCH_2), 2.60 (br s, 2H, two NH), and 1.13 (t, $^3J_{HH}$ = 7 Hz, 6H, two CH_3). ^{13}C NMR ($CDCl_3$) δ 197.6 ($C=O$), 136.7, 133.5, 128.8, and 128.2 (aromatic), 60.36 (d, $^2J_{CP}$ = 4 Hz, CH_2O), 39.39 (d, $^3J_{CP}$ = 7 Hz, $CH_2C=O$), 36.17 (NCH_2), and 17.78 (d, $^3J_{CP}$ = 7 Hz, CH_3). ^{31}P NMR ($CDCl_3$) δ 15.8 (relative to external 25% H_3PO_4 capillary in $CDCl_3$).

Synthesis of d-IPM

Under an atmosphere of nitrogen, a solution of benzyl alcohol (20 mmol, 2.07 ml) and triethylamine (20 mmol, 2.79 ml) in THF (dried/distilled, 20 ml) was added dropwise to a solution of phosphorus oxychloride (20 mmol, 1.87 ml) in THF (30 ml) which had been cooled to −23°C (CCl_4/dry ice). Following complete addition, the reaction mixture was stirred for 30 min. The bath was then changed to ethylene glycol/dry ice (−16°C) and a solution of ethylamine (80 mmol, 40 ml of a 2 *M* solution in THF) was added slowly to the reaction mixture using a syringe. After stirring for 1 h at low temperature, water (20 ml) was added to the mixture and then the THF was removed on a rotary evaporator. The resultant aqueous layer was extracted with CH_2Cl_2 (3×50 ml). The combined organic layers were dried ($MgSO_4$), filtered and concentrated on a rotary evaporator. The residual material was flash chromatographed on silica gel (230–400 mesh, 5.6×21 cm column) using ethyl acetate (approximately 800 ml) to remove faster eluting impurities and 10% ethanol in ethyl acetate to elute the product (R_f 0.58 in 10% ethanol/ethyl acetate). *N*,*N*′-Diethylphosphorodiamidic acid phenyl methyl ester [$C_6H_5CH_2OP(O)(NHCH_2CH_3)_2$] was obtained as an oil in 28% yield (1.33 g, 5.5 mmol). ^{1}H NMR ($CDCl_3$) δ 7.40–7.27 (m, 5H, aromatic), 4.99 (d, $^3J_{HP}$ = 7.7 Hz, 2H, OCH_2), 3.03–2.83 (brm, 4H, two NCH_2), 2.60–2.40 (br s, 2H, two NH), and 1.11 (dt, $^3J_{HH}$ = 7 Hz, $^4J_{HP}$ = ~1 Hz, 6H, two CH_3). ^{13}C NMR ($CDCl_3$) δ 137.0, 128.3, 127.9, and 127.5 (aromatic), 66.42 (d, $^2J_{CP}$ = 4.6 Hz, OCH_2), 35.95 (NCH_2), and 17.50 (d, $^3J_{CP}$ = 6.6 Hz, CH_3). ^{31}P NMR ($CDCl_3$) δ 16.3 (relative to external 25% H_3PO_4 capillary in $CDCl_3$).

N,*N*′-Diethylphosphorodiamidic acid phenyl methyl ester (5.5 mmol, 1.33 g) was dissolved in 6% 1,4-cyclohexadiene in absolute ethanol (230 ml) and this solution was passed through a column (1×6 cm) of palladium black at a rate of about 1 ml/min [28]. The collected solution was concentrated at room temperature on a rotary evaporator. The resultant oil was dissolved in ethanol using minimal warming. Upon complete dissolution, ether (75 ml) was added and the flask was stoppered and stored overnight at −20°C. The supernatant was decanted from the resultant crystals and the crystals were washed several times with ether. After drying under a stream of nitrogen, the product was obtained as a white microcrystalline solid in 33% yield (0.28 g, 1.8 mmol, m.p. 127–130°C). For the purposes of elemental analysis, the product was recrystallized using ethanol/ether. Analysis calculated for $C_4H_{13}N_2O_2P$, theory (found): C, 31.57 (31.71); H, 8.63 (8.55); N, 18.41 (18.58). ^{1}H NMR (D_2O/TSP) δ 2.91 (dq, $^3J_{HH}$ = 7 Hz, $^3J_{HP}$ = 8 Hz, 4H, two NCH_2) and 1.14 (dt, $^3J_{HH}$ = 7 Hz, $^4J_{HP}$ = ~1 Hz, 6H, two CH_3). ^{13}C NMR (D_2O/TSP) δ 39.42 (NCH_2) and 18.40 (d, $^3J_{CP}$ = 8 Hz, CH_3). ^{31}P NMR (0.01 *M* phosphate in D_2O, pD 7.0) δ 11.0 (with the solution phosphate at δ 2.1).

Kinetics

As summarized in Table 1, the half-life of each compound was measured at 37°C, pH 7.4, by ^{31}P NMR using methods described previously [29]. Linear least-squares fits of pseudo-first-order plots of the disappearance of appropriate ^{31}P signals provided rate constants and half-lives. ^{31}P NMR chemical shifts were referenced to external 25% H_3PO_4. Values of pH corresponded to observed readings and were uncorrected for deuterium isotope effects. Kinetic runs were considered valid if the pH varied by not more than 0.2 units over the course of spectral accumulation. Methylphosphonate was added to each NMR sample as an internal standard.

4HDI

Two kinetic runs for 4HDI (0.042 mmol) in 1 *M* lutidine (2,6-dimethylpyridine, 1.35 ml) and D_2O (0.15 ml) were completed. Spectra were acquired at 30-min intervals. For 4HDI (δ 11.8), the apparent rate constant was 0.0018 ± 0.0001 min^{-1} and the apparent half-life was 397 ± 12 min (correlation coefficient 0.998 ± 0.001).

Didechloro-(4-HO-IF/AIF)

The didechloro analogs of 4-HO-IF and AIF (i.e., didechloro-4-HO-IF and didechloro-AIF) were generated in situ by the thiosulfate reduction of 4HDI, as has been reported for the reduction of 4-HI and related compounds [29, 30]. An NMR sample of 4HDI (0.034 mmol) was prepared using 1 *M* lutidine (1.35 ml) and D_2O (0.15 ml) and to this was added, slowly, sodium thiosulfate pentahydrate (0.136 mmol, 34 mg). The solution pH was adjusted to 7.4 and spectra were acquired at 10-min intervals. Kinetic data for half-life determinations were based on spectral data acquired after the interconverting *cis*- and *trans*-hydroxy and aldehydic species had come to a pseudo-equilibrium (approximately 20 min at 37°C) [29, 30]. At pseudo-equilibrium, the average relative ratio of didechloro-*cis*-4-HO-IF (δ 13.3) to didechloro-*trans*-4-HO-IF (δ 12.9) to didechloro-AIF (and its hydrate, δ 19.0) was constant at 43:50:7. As an average of two kinetic experiments for didechloro-(4-HO-IF/AIF), the apparent rate constant was 0.0073 ± 0.0002 min^{-1} and the apparent half-life was 96 ± 2 min (correlation coefficient 0.998 ± 0.001). (*Note*: Interconverting species, such as the hydroxy and aldehydic species discussed here, are characterized by an 'apparent' half-life in that the rate of disappearance for each species appears the same [29, 30].)

Table 1 ^{31}P NMR-derived half-lives at 37 ± 2°C, pH 7.4 ± 0.2 (*PVK* phenylvinylketone)

Compound (→ products)	Half-life	Conditions[a]
4HI (→ 4HO-IF/AIF)	14 h[b]	23 m*M* in 0.9 *M* lutidine
4HDI (→ didechloro-4HO-IF/AIF)	6.6 ± 0.2 h	23 m*M* in 0.9 *M* lutidine
4HC (→ 4HO-CP/AP)	89 min[c]	23 m*M* in 0.9 *M* lutidine
4HDC (→ didechloro-4HO-CP/AP)	101 min[c]	28 m*M* in 0.9 *M* lutidine
4HO-IF/AIF (→ acrolein + IPM)	44 min[d]	20 m*M* in 0.9 *M* lutidine
Didechloro-4HO-IF/AIF (→ acrolein + d-IPM)	96 ± 2 min	23 m*M* in 0.9 *M* lutidine
4HO-CP/AP (→ acrolein + PM)	38 min[e]	20 m*M* in 0.9 *M* lutidine
Didechloro-4HO-CP/AP (→ acrolein + d-IPM)	50 min[c]	23 m*M* in 0.9 *M* lutidine
PKIF (→ PVK + IPM)	63 min[f]	20 m*M* in 1 *M* lutidine/DMSO (8:2)
d-PKIF (→ PVK + d-IPM)	61 ± 1 min	20 m*M* in 1 *M* lutidine/DMSO (8:2)
4HO-CP/AP (→ acrolein + PM)	69 min[f]	20 m*M* in 1 *M* lutidine/DMSO (8:2)
PM	20 min (16 min)[d,g]	17 m*M* in 0.9 *M* lutidine
IPM	81 min (167 min)[d,g]	17 m*M* in 0.9 *M* lutidine
d-IPM	1–2 months[h]	33 m*M* in 0.33 *M* bisTris

[a]Half-lives for these compounds are dependent on conditions, including pH, temperature, buffer, chloride concentration and/or nucleophiles present in solution [44]
[b]Taken from reference 44
[c]Taken from reference 45
[d]Taken from reference 30
[e]Taken from reference 29
[f]Taken from reference 26
[g]Number in parentheses relates to the rate of the second alkylation step
[h]Based on 10–15% loss of d-IPM after 8 days

d-PKIF

As has been described for the kinetics of PKIF [26], d-PKIF (0.034 mmol) was dissolved in DMSO-d_6 (0.34 ml) and then diluted with 1 *M* lutidine (1.35 ml). Sodium thiosulfate pentahydrate (0.136 mmol, 34 mg) was added and the solution pH was adjusted to 7.4. (*Note*: Thiosulfate was added so as to mimic the conditions/dielectric constant of previous kinetic samples of PKIF. The thiosulfate had no other chemical function in this sample.) Spectra were acquired at intervals of 10 min. As an average of two kinetic runs for d-PKIF (δ 21.9), the rate constant was 0.0114 ± 0.0001 min^{-1} and the half-life was 61 ± 1 min (correlation coefficient 0.998 ± 0.001).

d-IPM

d-IPM (0.16 mmol) was dissolved in 1 *M* bisTris and this was diluted with H_2O (2.85 ml) and D_2O (0.5 ml). Spectra were acquired initially at 15-min intervals, followed by hourly and then daily intervals over 8 days. After 8 days, the loss of d-IPM (δ 14.2) was approximately 10–15%. This led to the calculation of an estimated half-life of approximately 1–2 months.

Construction of plasmids and cell transfection

The wild-type *agt* gene was amplified and constructed as described previously [23]. CHO cells were transfected with either pcDNA3 or wtAGT (pcDNA3 plasmid containing cDNA for wild-type AGT) via electroporation [31]. Briefly, CHO cells were grown to about 60% confluence, trypsinized, washed once with HEPES buffer (10 m*M*), followed by resuspension in HEPES buffer at 1×10^7 cells/ml. A 400-µl aliquot of the cell suspension was then mixed with 40 µg of DNA in an electroporation cuvette (2 mm gap size) and electroporated for about 5 ms at 870 V/cm (400 µF, 13 Ω internal resistance) on a BTX ECM 600 electroporator (Genetronics Biomedical, San Diego, Calif.). Electroporated cells were held on ice for 10 min before plating out in growth medium. After 24 h, the medium was replaced with G418-containing growth medium and the cells grown for 10–12 days. Individual colonies were then trypsinized and grown to a larger scale for AGT activity screening. We have previously shown that AGT activity in CHO^{pcDNA} is negligible compared to CHO^{wtAGT} cells, thus providing an effective control system to evaluate the effects of AGT [32].

Triphenylphosphine reduction of 4HI and 4HDI

In solution, 4HI and 4HDI spontaneously convert to hydroxy metabolites; however, the half-lives for these reactions can be relatively long (12–16 h), depending on conditions (Table 1). Thus, both 4HI and 4HDI were pre-reduced to hydroxy metabolites prior to cell treatment as described previously [24]. Briefly, 4HI or 4HDI (5 mg) was dissolved in 3 ml CH_2Cl_2 prior to the addition of triphenylphosphine (3.57 mg triphenylphosphine per milligram 4HI or 4HDI). This solution was stirred at 5°C for 10 min and the organic layer evaporated under a constant nitrogen stream. Sterile water (2 ml) was added to the precipitate which was followed by vortexing vigorously for 5 min. This slurry was then filter-sterilized through a 0.2-µm filter just prior to cell treatment. The filtrate, which was an aqueous solution of reactive hydroxy/aldehydic metabolites, was used immediately. The reduction of 4HI and the extraction of the resultant metabolites into water has been shown to be quantitative [24].

Assay for cell survival

The cytotoxicity induced by 4HI, 4HDI, IPM, PKIF, d-IPM, d-PKIF and CAA was determined by loss of colony-forming ability as described previously [32]. All survival assays were performed at 37°C. Briefly, CHO cells transduced with pcDNA3 or wtAGT were plated at a density of 1.4×10^6 cells/T75 flask. The medium was changed to serum-free DMEM 16–18 h later and cells were exposed to either BG (100 µ*M*) or vehicle alone (0.01% DMSO) for 2 h. The cells were then treated with increasing concentrations of pre-reduced 4HI, pre-reduced 4HDI, IPM, PKIF, d-IPM, d-PKIF or CAA for 2 h. All drug solutions were prepared immediately prior to use on the day of treatment. PKIF and d-PKIF were dissolved in DMSO and then diluted in medium to give solutions that were less than 0.01% DMSO; due to solubility, some d-PKIF solutions and respective controls contained up to 2.5% DMSO. All control solutions contained the same amount of DMSO as the respective treatment group. After drug washout and replacement with fresh DMEM plus serum, cells that were pretreated with BG were incubated overnight in medium with continued exposure to 100 µ*M* BG. CHO cells were subsequently plated at a density of 200–1000 cells/dish and allowed to undergo exponential growth for 10–12 days prior to counting colonies. Colonies were counted after staining with methylene blue, and survival of colony-forming efficiency was

expressed as a percentage of the appropriate set of control cells exposed to vehicle alone.

Assay for determining apoptosis in CHO cells

Cells were treated according to the treatment schema described above for cell survival with 200 μ*M* IPM and analyzed for percent apoptotic cells at various time-points. All apoptosis assays were performed at 37°C. Cells were treated with increasing concentrations of IPM (100, 200, 300 μ*M*) and analyzed for percent apoptosis at 72 h post-treatment. At 0–96 h following treatment with IPM, cells were harvested via trypsinization and washed with DMEM supplemented with 10% FBS. A minimum of 1×10^6 cells were then costained with annexin V and PI. Samples were analyzed by FACS for annexin-positive and PI-negative cells. Percent apoptosis was defined as the percent of annexin-positive and PI-negative cells compared to the total number of cells in the analysis sample and in the corresponding control sample.

Assay for cell cycle distribution of CHO cells

Cells were treated with either 200 μ*M* IPM for 2 h, 10 μ*M* PKIF for 2 h, or 300 μ*M* PM for 1 h in the presence and absence of BG as described above for cell survival studies. All cell cycle distribution assays were performed at 37°C. PM was prepared in phosphate buffer solution immediately prior to cell exposure. At 0, 16 and 24 h following the end of treatment, cells were harvested and fixed in ice-cold alcohol for FACS analysis. Harvested cells were centrifuged at 1200 rpm for 5 min with two wash steps prior to resuspending the pellet in PBS. Cells were then fixed in 75% ice-cold ethanol and refrigerated for at least 30 min prior to analysis. Cells were stained in a PI solution containing RNase at a final concentration of approximately 1×10^6 cells/ml. Flow cytometric analysis was performed using FACScan (Becton Dickinson, Franklin Lakes, N.J.).

Results

Compounds used in this study

Previous data from our laboratory indicate that BG increases the sensitivity of CHO cells to 4HC and PM [23]. To extend these observations, we investigated the effect of BG on the sensitivity of CHO cells overexpressing AGT activity treated with ifosfamide and its metabolites (Fig. 1). Ifosfamide analogs were designed to selectively generate just one cytotoxic metabolite, acrolein or IPM, to allow specific evaluation of each metabolite in combination with BG.

A summary of pertinent products of the investigated compounds is shown in Fig. 1. Compounds investigated included 4HI (activated form of ifosfamide) as a source of acrolein and IPM through aqueous degradation to 4-HO-IF and AIF. To study the effects of acrolein, 4HDI was selected. Similar to 4HI, 4HDI was reduced with triphenylphosphine to ultimately produce acrolein and d-IPM (a nonalkylating analog of IPM). To isolate the effects of IPM, authentic material was used; however, IPM has relatively poor cellular uptake and, therefore, high concentrations are required for in vitro activity. PKIF seems to have better membrane permeability and is capable of generating IPM intracellularly. Thus, PKIF was also used in this study. PKIF is most appropriately viewed as an analog of AIF since it undergoes a spontaneous and direct fragmentation to IPM and the acrolein analog phenylvinylketone. In control experiments, the nontoxic effects of d-IPM and phenylvinylketone were verified using synthetic d-IPM and d-PKIF (fragments to d-IPM and phenylvinylketone) (data not shown). Because none of the analogs used would generate CAA, authentic CAA was used to study the effects of this metabolite. The relative kinetic characteristics of the conversions discussed above are shown in Table 1.

Effect of BG alone on cytotoxicity in CHO cells expressing AGT and vector control

The dose of BG used in all cytotoxicity experiments was 100 μ*M* for 2 h prior to, during and 16 h following alkylating agent. In our previous studies [33] we found that this dose of BG in CHO cells results in approximately 10% decreased cell survival relative to control, although the standard deviations show overlapping values. An analysis of eight to ten experiments indicated 11% and 16% decrease in cell survival in BG-treated wtAGT and pcDNA cells, respectively. Grossly, colonies exposed to BG alone were qualitatively smaller than, but quantitatively not significantly different from, respective colonies on the control plates (data not shown).

Effect of BG on ifosfamide-induced cytotoxicity in CHO cells expressing AGT and vector control

To ascertain the contribution of AGT inactivation by BG, CHO cells were transfected with wild-type AGT and plasmid. As shown in Fig. 2 (top panel), 100 μ*M* BG substantially enhanced the sensitivity of CHO^{wtAGT} cells to cytotoxicity induced by 4HI, IPM, and PKIF, but not that induced by 4HDI or CAA. The addition of BG decreased the IC_{90} of 4HI, IPM, and PKIF as summarized in Table 2. In contrast, BG did not affect cytotoxicity caused by 4HDI or CAA. Taken together, BG enhanced the IPM metabolite of 4HI, but not acrolein or CAA metabolites.

To determine if the enhanced toxicity caused by BG exposure was mediated by inactivation of AGT, each compound related to ifosfamide was next tested for toxicity in CHO^{pcDNA} cells in the presence and absence of BG (Fig. 2, bottom panel). This cell line has undetectable AGT activity [23]. Similar to results in CHO^{wtAGT} cells, BG enhanced the sensitivity of CHO^{pcDNA} cells to 4HI, IPM, and PKIF (Table 2), but not to 4HDI and CAA, ruling out AGT inactivation by BG as the mechanism of enhancement of these agents.

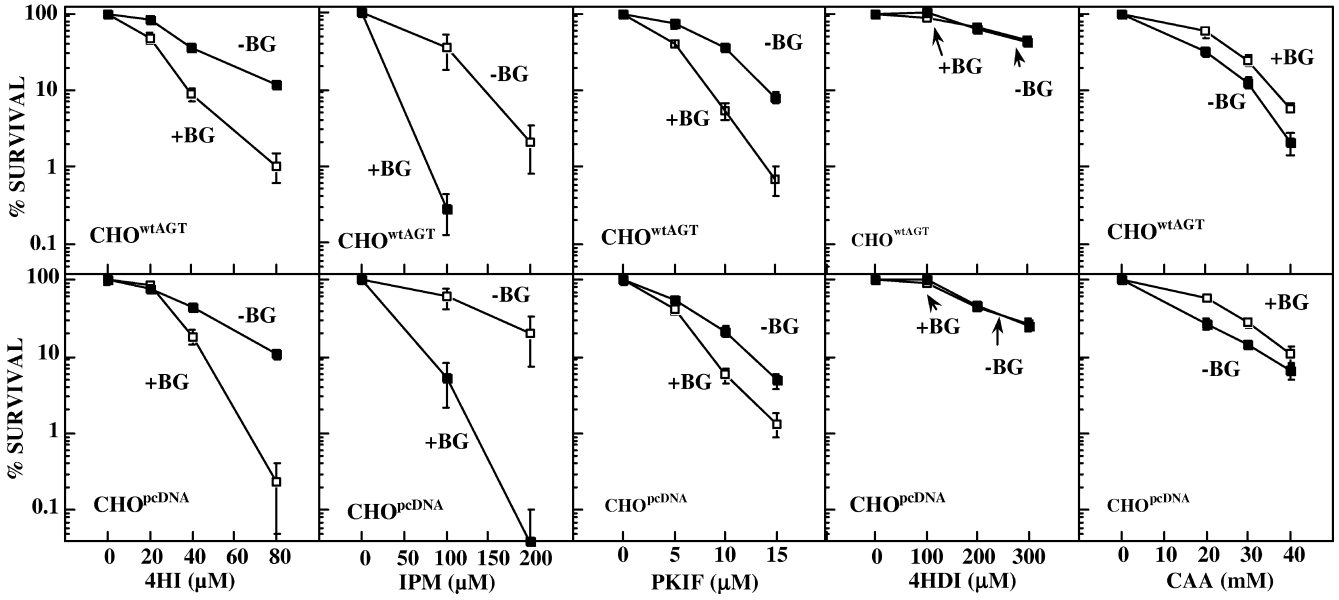

Fig. 2 Effect of BG on cytotoxicity induced by compounds related to ifosfamide. CHO^{wtAGT} cells or CHO^{pcDNA} were treated with 100 μ*M*BG (□) or vehicle (0.01% DMSO, ■) for 2 h prior to, during and 16–18 h following treatment with ifosfamide metabolites or analogs that generate select metabolites (reduced 4HI, PKIF, IPM, reduced 4HDI, CAA). Each data point represents the mean ± SD from three to five separate experiments (except CAA where $n = 2$). Each experiment represents five replicate dishes per treatment group

Effect of BG on the sensitivity of cells to d-IPM and d-PKIF

Due to the anionic nature of IPM at pH 7.4 which results in poor membrane permeability [24, 30], high concentrations were necessary for cell toxicity experiments (Fig. 2). Therefore PKIF was employed as a generator of IPM (Fig. 1). As discussed above, the toxicity induced by PKIF was enhanced by BG in both CHO^{wtAGT} and CHO^{pcDNA} cells (Fig. 2). A byproduct of PKIF is phenylvinylketone. Therefore, to rule out any effect by the byproduct, d-PKIF (produces d-IPM and phenylvinylketone) and d-IPM were studied. BG did not have any effect on the toxicity of these agents (data not shown). These data, together with the finding that BG had no effect on the toxicity of 4HDI, further suggest that the effect of BG on 4HI-induced cytotoxicity is related solely to the IPM product.

Effect of BG on apoptotic cell death in CHO cells treated with IPM

The mechanism by which BG enhances cytotoxicity in the absence of AGT is not known but may involve programmed cell death. To determine if cells exposed to the combination of BG and IPM follow an apoptotic pathway, an annexin V-FITC and PI assay was performed at various time-points following the end of treatment with 200 μ*M* IPM in the presence and absence of BG. The difference in percent apoptosis was most dramatic at 72 h (Fig. 3A). We further investigated percent apoptosis with different doses of IPM with or without BG at the 72-h time-point (Fig. 3B). The addition of BG to 200 μ*M* IPM increased the percent of apoptotic cells from 5.5 ± 2.8% to 38 ± 7.1% (Fig. 3B).

Effect of BG on cell cycle distribution following treatment with IPM, PKIF or PM

We reasoned that the observed BG-enhanced IPM toxicity might be related to the effect of BG on the proportion of cycling versus noncycling cells, ultimately altering the sensitivity of cells to the crosslinking agent. Our thinking was based on an earlier observation that nitrogen mustards are more toxic in noncycling than in cycling cells [34]. We evaluated cell cycle kinetics following treatment with IPM, PKIF and PM (crosslinking

Table 2 IC_{90} of 4HI, IPM and PKIF in CHO cells in the presence and absence of BG. The addition of BG decreased the IC_{90} of all three compounds in both wtAGT and pcDNA CHO cell lines

Compound	IC_{90} (μ*M*)					
	wtAGT			pcDNA		
	Without BG	With BG	Fold difference	Without BG	With BG	Fold difference
4HI	> 80	39	2.1	> 80	45	1.8
IPM	145	39	3.7	> 200	77	2.6
PKIF	14	8	1.8	12	9	1.3

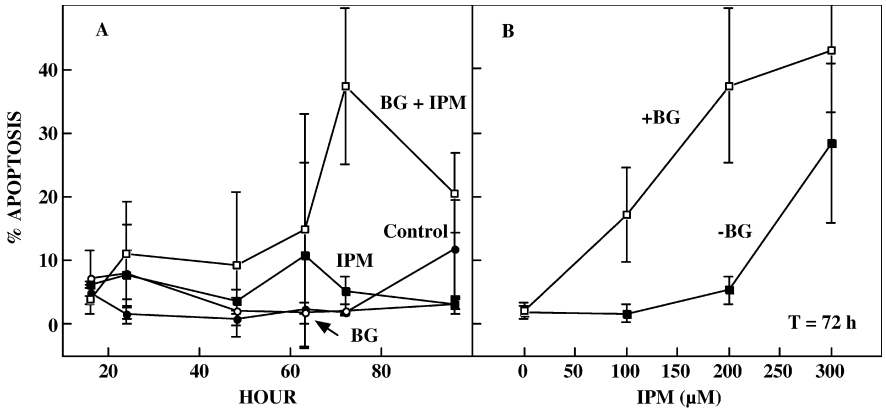

Fig. 3A, B Effect of BG on apoptotic cell death in CHO cells following treatment with IPM using an annexin V-FITC assay. **A** CHO cells were treated with 100 μ*M* BG vs vehicle (0.01% DMSO) for 2 h prior to, during and 16–18 h following treatment with 200 μ*M* IPM for 2 h. Between 0 and 96 h later, the percentage of cells undergoing apoptosis was determined. **B** At 72 h following treatment with IPM (100, 200, 300 μ*M*), in the presence and absence of BG, cells were analyzed by flow cytometry for apoptosis. Each data point represents the mean ± SD of three separate experiments

metabolite of cyclophosphamide) in the presence and absence of BG. Immediately following treatment (0 h), there was no change in cell cycle distribution between control and treated cells with approximately one-third to one-half of cells in G_1 across all treatment groups (Fig. 4, top panel). However, at 16 h, cells exposed to BG were primarily in G_1 (78%) whereas significantly fewer cells were in G_1 following treatment with vehicle, IPM, PKIF or PM (Fig. 4, bottom panel). Specifically, of cells treated with IPM alone versus IPM plus BG, the percent in G_1 increased from 16% to 29%. The difference was even more dramatic for cells treated with PKIF and PM in which the percent cells in G_1 increased from 20% to 64% and 18% to 51%, respectively, with the addition of BG. Flow data at 16 h from a representative experiment are shown in Fig. 5. The effect on cell cycle distribution persisted but was slightly decreased at 24 h and was absent at 48 h (data not shown).

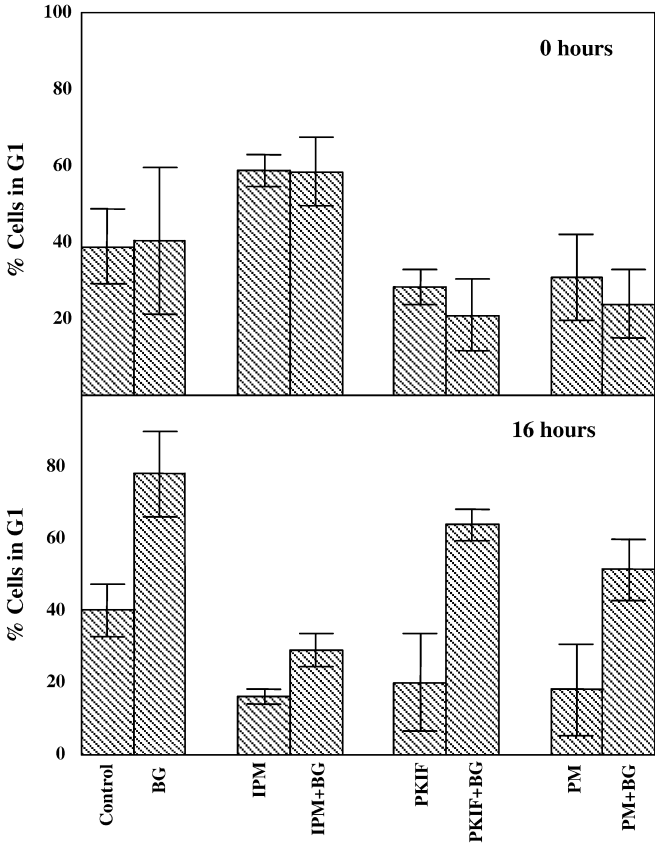

Fig. 4 Effect of BG on percentage of cells in G_1. CHO cells were treated with 200 μ*M* IPM, 10 μ*M* PKIF or 300 μ*M* PM. At 0 and 16 h following the end of treatment, cells were harvested and fixed for FACS analysis. Each bar represents the mean ± SD from three to seven separate experiments

Discussion

Our results show that BG has a mechanism of action distinct from AGT inhibition. This was demonstrated by its enhancement of ifosfamide-induced cytotoxicity in CHO cells devoid of AGT activity. The increased cytotoxicity occurred in the context of increased cellular apoptosis and blockade of cell cycle progression with G_1 arrest. Whether or not the increased cytotoxicity occurs as a consequence of cell cycle arrest is of great interest and forms the basis for ongoing investigations. The significance of these findings is that BG, a nontoxic compound already in clinical trials, can be combined with ifosfamide to increase the toxicity exerted by IPM, the ifosfamide metabolite thought to contribute primarily to the antitumor effect. Conversely, there was no increase in the cytotoxicity associated with CAA, the metabolite responsible for neurotoxicity, or reduced 4HDI, an analog producing the urotoxic metabolite, acrolein. Thus, the combination of BG with nitrogen mustards such as ifosfamide may allow lower total doses with a resultant decrease in clinically relevant toxicity without compromising efficacy. Confirmation of the current results in human cell lines as well as in vivo models is actively being pursued.

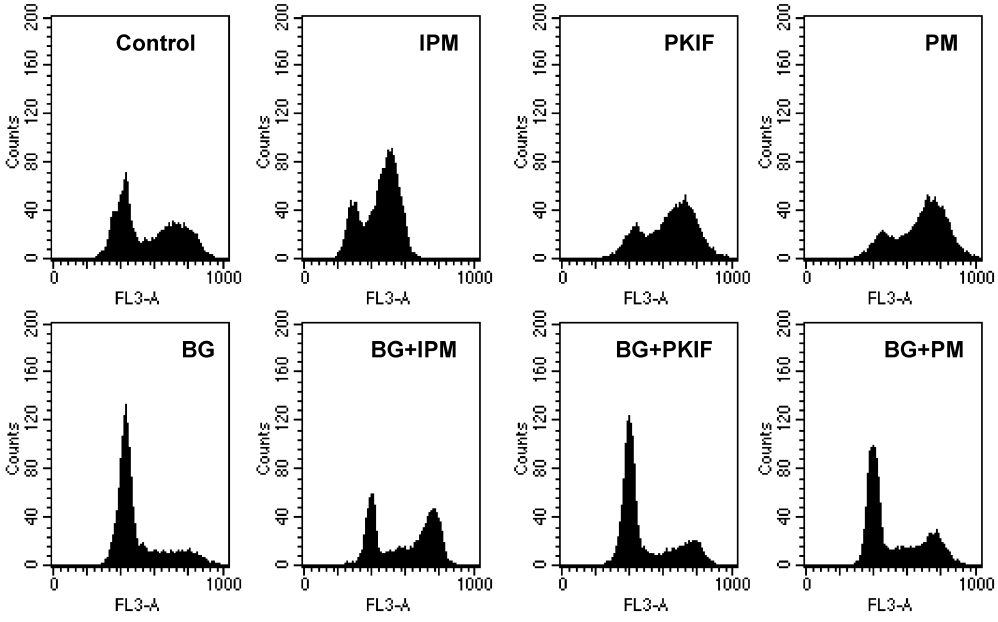

Fig. 5 Flow cytometric analysis of cell cycle distribution at 16 h following treatment with IPM, PKIF, and PM with or without BG. CHO cells were treated with 200 μ*M* IPM, 10 μ*M* PKIF or 300 μ*M* PM. Histograms are from representative experiments

BG was originally designed as a specific, potent inactivator of the DNA repair protein, AGT. In this capacity, BG acts to enhance the toxicity of nitrosoureas and alkyltriazenes by increasing the number of lesions at the O^6-position of guanine. A consequence of persistent O^6-adducts is increased toxicity and mutagenicity. In contrast, the effect of BG combined with ifosfamide appears to be AGT-independent, and therefore would not be expected to be associated with production of mutagenic O^6-adducts. Furthermore, the associated increase in apoptosis in our experiments would also serve to decrease the likelihood that mutagenic lesions would persist during DNA replication. These results are consistent with previous results in CHO cells from our laboratory demonstrating effective modulation of 4HC, PM, chlorambucil, and melphalan by BG [23, 33]. In these analyses, the addition of BG to PM resulted in decreased mutagenicity as measured by *hprt* mutant colonies. Finally, only the metabolite thought to cause the antitumor effect (IPM) is enhanced, as compared to the nitrosoureas where the addition of BG results in increased toxicity concomitant with increased mutagenicity.

The concentration of BG used to enhance BCNU and other alkylnitrosoureas is in the submicromolar range compared to 100 μ*M* BG used in the present study for enhancement of ifosfamide metabolites. This is because BG was designed as a potent, selective inactivator of AGT. We have observed an enhancement of cyclophosphamide-mediated cytotoxicity in CHO cells at concentrations as low as 10 μ*M* BG for 4 h (unpublished data); however, the enhancement is less than the enhanced cytotoxicity seen with higher doses of BG and longer exposure times. At the phase II dose of BG (120 mg/m^2 given over 1 h) in humans, the maximal plasma concentrations of BG and 8-oxoBG, an equally effective metabolite, are 4 μ*M* and 28 μ*M*, respectively. Although BG alone is not toxic to humans at this dose level [35], it is likely that higher dose levels and longer infusion times would be required for effective modulation of ifosfamide at a clinical level. Determining the cellular target(s) of BG responsible for ifosfamide enhancement will allow the design of more potent modulators.

Our data showed that treatment with BG, both alone and in combination with ifosfamide derivatives, arrested exponentially growing CHO cells in G_1. The contributory effect of ifosfamide on cell cycle kinetics in CHO cells appeared to be accumulation in S phase or G_2/M (Fig. 5). Others have also shown that nitrogen mustards inhibit cells at G_2/M [36, 37]. However, the cell cycle influence of nitrogen mustards appears to differ among cell lines, since others have shown accumulation of cells in other portions of the cell cycle [36, 38]. Regardless, in our studies, IPM did not cause accumulation of cells in G_1 unless given with BG. Although there appeared to be an effect of BG on cell cycle kinetics and on the toxicity of DNA crosslinking agents, we did not unequivocally show that these two effects are related. In support of our data, others have shown that cell populations enriched in G_1 are more sensitive to nitrogen mustards than those enriched in late S phase or G_2 [34]. De Silva et al. have recently demonstrated that repair of ICLs produced by nitrogen mustards in stationary phase results in few double strand breaks as compared to a significant level in nonstationary phase cells [19]. They proposed that repair of ICLs in dividing cells involves the formation of double strand breaks at stalled replication forks that initiate homologous recombination followed by excision repair [19]. Cell cycle distribution may alter the response to nitrogen mustards by differential repair of DNA crosslinks in cycling versus noncycling mammalian cells.

The repair of DNA crosslinks is complex and not fully understood; however, proteins belonging to both excision repair and recombination pathways are involved [19, 39, 40]. It is possible that differences in damage recognition or repair of DNA crosslinks in G_1 versus S dictate growth arrest or apoptosis at a cellular level.

A recent investigation into substituted guanines has revealed that certain O^6-alkylguanines including BG have potent CDK-inhibitory activity [41, 42, 43]. The O^6-alkylguanine compounds appear to be relatively selective for the ATP binding site of CDK1 and CDK2. An analysis of structure-activity relationships suggests that the main influence of the specific O^6-substituent is on potency of CDK inhibition [43]. The IC_{50} for BG-mediated inhibition of CDK1/cyclin B and CDK2/cyclin A was 24 ± 3 μM and 35 ± 6 μM. Thus it is likely that in our experiments both CDK1 and CDK2 were inhibited by BG, explaining G_1 arrest [43].

Recently, we have demonstrated that the AGT protein plays a role in resistance to acrolein [32], a metabolite common to both cyclophosphamide and ifosfamide. Cells overexpressing AGT were resistant to the toxic and mutagenic effects of 4HDC (forms acrolein and nonalkylating PM) compared to control cells. Upon treatment of CHO^{wtAGT} with BG, there was an increase in sensitivity of cells to 300 μM 4HDC, although no difference was demonstrated at lower doses [23]. Our present data do not show increased sensitivity of CHO^{wtAGT} to 300 μM pre-reduced 4HDI upon treatment with BG as might be expected if AGT is repairing an acrolein adduct on DNA. There are several aspects that may account for the different effects of BG on 4HDI-derived versus 4HDC-derived acrolein. First, we considered whether or not comparable amounts of acrolein were being generated in each of the experiments. Because we pre-reduced the 4HDI, acrolein generation was based only on the rate of decomposition of the hydroxy/aldehydic metabolites (didechloro-4-HO-IF/AIF). In contrast 4HDC was not pre-reduced and, therefore, the kinetics of two steps had to be considered: (1) 4HDC $\rightarrow$ didechloro-4-HO-CP/AP; and (2) didechloro-4-HO-CP/AP $\rightarrow$ acrolein. Of these two steps, the first would be rate-limiting (Table 1). Considering the half-lives for the pertinent reactions, the rate of production of acrolein from reduced 4HDI and from 4HDC would be nearly the same under similar conditions (Table 1), even though it is based on rate constants determined in buffers not cells. It is possible that the reduction of 4HDC would be rapid if peroxidases were present and, therefore, no longer rate-limiting. This results in different amounts of acrolein which may account for the disparity in the experimental results. Second, our previous study extended BG treatment (10 μM) for an additional 10 days. The CHO^{wtAGT} cells used in both studies have extremely high AGT activity (1432 fmol/mg protein) as a result of the use of a strong promoter; even in the presence of 100 μM BG for 24 h, 10% of AGT activity is expressed [23]. It is likely that this residual activity may be enough to repair any potential O^6-guanine adducts being generated from reduced 4HDI or lower doses of 4HDC. The longer exposure time of BG in the 4HDC experiment would be expected to result in depletion of residual AGT and newly synthesized AGT, explaining the enhancement with 4HDC.

In summary, we have shown that BG influences ifosfamide-mediated toxicity in CHO cells in a novel way. BG increases the toxicity of 4HI and its major crosslinking metabolite, IPM, by enhancing apoptosis possibly through a mechanism involving G_1 arrest. The potential impact of selective enhancement of IPM and not acrolein or CAA by BG is improved antitumor activity without increased toxicity associated with metabolites that are not thought to contribute to the antitumor effect. The findings of the present study compellingly support further investigation into the mechanism of action of BG in order to design more potent modulators. The prospect that a nontoxic compound such as BG can increase the toxicity of a commonly used alkylating agent such as ifosfamide expands the range of potentially beneficial applications for patients with malignant diseases, and further preclinical and clinical investigation is warranted.

References

1. Reiser M, Bredenfeld H, Engert A, Diehl V (2001) The role of ifosfamide in the treatment of relapsed and refractory lymphoma. Eur J Haematol Suppl (64):37–40
2. Sambrook RJ, Girling DJ (2001) A national survey of the chemotherapy regimens used to treat small cell lung cancer (SCLC) in the United Kingdom. Br J Cancer 84:1447–1452
3. Vokes EE, Hoffman PC, Masters GA, Golomb HM, Drinkard LC, Krauss SA (1996) Ifosfamide-based chemotherapy for non-small cell lung cancer: phase I/II studies at the University of Chicago. Semin Oncol 23:15–18
4. Dechant KL, Brogden RN, Pilkington T, Faulds D (1991) Ifosfamide/mesna. A review of its antineoplastic activity, pharmacokinetic properties and therapeutic efficacy in cancer. Drugs 42:428–467
5. Nielsen OS, Judson I, Van Hoesel Q, Le Cesne A, Keizer HJ, Blay JY, van Oosterom A, Radford JA, Svancarova L, Krzemienlecki K, Hermans C, Van Glabbeke M, Oosterhuis JW, Verweij J (2000) Effect of high-dose ifosfamide in advanced soft tissue sarcomas. A multicentre phase II study of the EORTC Soft Tissue and Bone Sarcoma Group. Eur J Cancer 36:61–67
6. Schneider DT, Hilgenfeld E, Schwabe D, Behnisch W, Zoubek A, Wessalowski R, Gobel U (1999) Acute myelogenous leukemia after treatment for malignant germ cell tumors in children. J Clin Oncol 17:3226–3233
7. Kaijser GP, Korst A, Beijnen JH, Bult A, Underberg WJ (1993) The analysis of ifosfamide and its metabolites (review). Anticancer Res 13:1311–1324
8. Williams ML, Wainer IW (1999) Cyclophosphamide versus ifosfamide: to use ifosfamide or not to use, that is the three-dimensional question. Curr Pharm Des 5:665–672
9. Yu L, Waxman DJ (1996) Role of cytochrome P450 in oxazaphosphorine metabolism. Deactivation via N-dechloroethylation and activation via 4-hydroxylation catalyzed by distinct subsets of rat liver cytochromes P450. Drug Metab Dispos 24:1254–1262
10. Brock N, Stekar J, Pohl J, Niemeyer U, Scheffler G (1979) Acrolein, the causative factor of urotoxic side-effects of cyclophosphamide, ifosfamide, trofosfamide and sufosfamide. Arzneimittelforschung 29:659–661

11. Mohrmann M, Ansorge S, Schmich U, Schonfeld B, Brandis M (1994) Toxicity of ifosfamide, cyclophosphamide and their metabolites in renal tubular cells in culture. Pediatr Nephrol 8:157–163
12. Bruggemann SK, Kisro J, Wagner T (1997) Ifosfamide cytotoxicity on human tumor and renal cells: role of chloroacetaldehyde in comparison to 4-hydroxyifosfamide. Cancer Res 57:2676–2680
13. Pelgrims J, De Vos F, Van Den BJ, Schrijvers D, Prove A, Vermorken JB (2000) Methylene blue in the treatment and prevention of ifosfamide-induced encephalopathy: report of 12 cases and a review of the literature. Br J Cancer 82:291–294
14. Struck RF, Davis RL Jr, Berardini MD, Loechler EL (2000) DNA guanine-guanine crosslinking sequence specificity of isophosphoramide mustard, the alkylating metabolite of the clinical antitumor agent ifosfamide. Cancer Chemother Pharmacol 45:59–62
15. Dong Q, Barsky D, Colvin ME, Melius CF, Ludeman SM, Moravek JF, Colvin OM, Bigner DD, Modrich P, Friedman HS (1995) A structural basis for a phosphoramide mustard-induced DNA interstrand cross-link at 5′-d(GAC). Proc Natl Acad Sci U S A 92:12170–12174
16. Povirk LF, Shuker DE (1994) DNA damage and mutagenesis induced by nitrogen mustards. Mutat Res 318:205–226
17. Ojwang JO, Grueneberg DA, Loechler EL (1989) Synthesis of a duplex oligonucleotide containing a nitrogen mustard interstrand DNA-DNA cross-link. Cancer Res 49:6529–6537
18. Lawley PD, Phillips DH (1996) DNA adducts from chemotherapeutic agents. Mutat Res 355:13–40
19. De Silva IU, McHugh PJ, Clingen PH, Hartley JA (2000) Defining the roles of nucleotide excision repair and recombination in the repair of DNA interstrand cross-links in mammalian cells. Mol Cell Biol 20:7980–7990
20. Davis ST, Benson BG, Bramson HN, Chapman DE, Dickerson SH, Dold KM, Eberwein DJ, Edelstein M, Frye SV, Gampe RT Jr, Griffin RJ, Harris PA, Hassell AM, Holmes WD, Hunter RN, Knick VB, Lackey K, Lovejoy B, Luzzio MJ, Murray D, Parker P, Rocque WJ, Shewchuk L, Veal JM, Walker DH, Kuyper LF (2001) Prevention of chemotherapy-induced alopecia in rats by CDK inhibitors. Science 291:134–137
21. Dolan ME, Stine L, Mitchell RB, Moschel RC, Pegg AE (1990) Modulation of mammalian O6-alkylguanine-DNA alkyltransferase in vivo by O6-benzylguanine and its effect on the sensitivity of a human glioma tumor to 1-(2-chloroethyl)-3-(4-methylcyclohexyl)-1-nitrosourea. Cancer Commun 2:371–377
22. Dolan ME, Moschel RC, Pegg AE (1990) Depletion of mammalian O6-alkylguanine-DNA alkyltransferase activity by O6-benzylguanine provides a means to evaluate the role of this protein in protection against carcinogenic and therapeutic alkylating agents. Proc Natl Acad Sci U S A 87:5368–5372
23. Cai Y, Wu MH, Xu-Welliver M, Pegg AE, Ludeman SM, Dolan ME (2000) Effect of O6-benzylguanine on alkylating agent-induced toxicity and mutagenicity in Chinese hamster ovary cells expressing wild-type and mutant O6-alkylguanine-DNA alkyltransferases. Cancer Res 60:5464–5469
24. Boal JH, Ludeman SM, Ho CK, Engel J, Niemeyer U (1994) Direct detection of the intracellular formation of carboxyphosphamides using nuclear magnetic resonance spectroscopy. Arzneimittelforschung 44:84–93
25. Hales BF, Ludeman SM, Boyd VL (1989) Embryotoxicity of phenyl ketone analogs of cyclophosphamide. Teratology 39:31–37
26. Ludeman SM, Boyd VL, Regan JB, Gallo KA, Zon G, Ishii K (1986) Synthesis and antitumor activity of cyclophosphamide analogues. 4. Preparation, kinetic studies, and anticancer screening of "phenylketophosphamide" and similar compounds related to the cyclophosphamide metabolite aldophosphamide. J Med Chem 29:716–727
27. Takamizawa A, Matsumoto S, Iwata T, Makino I (1977) Synthesis, stereochemistry and antitumor activity of 4- hydroperoxyisophosphamide (NSC-227114) and related compounds. Chem Pharm Bull (Tokyo) 25:1877–1891
28. Springer JB, Colvin ME, Colvin OM, Ludeman SM (1998) Isophosphoramide mustard and its mechanism of bisalkylation. J Org Chem 63:7218–7222
29. Zon G, Ludeman SM, Brandt JA, Boyd VL, Ozkan G, Egan W, Shao KL (1984) NMR spectroscopic studies of intermediary metabolites of cyclophosphamide. A comprehensive kinetic analysis of the interconversion of cis- and trans-4-hydroxycyclophosphamide with aldophosphamide and the concomitant partitioning of aldophosphamide between irreversible fragmentation and reversible conjugation pathways. J Med Chem 27:466–485
30. Boal JH, Williamson M, Boyd VL, Ludeman SM, Egan W (1989) 31P NMR studies of the kinetics of bisalkylation by isophosphoramide mustard: comparisons with phosphoramide mustard. J Med Chem 32:1768–1773
31. Wahl GM, Lewis KA, Ruiz JC, Rothenberg B, Zhao J, Evans GA (1987) Cosmid vectors for rapid genomic walking, restriction mapping, and gene transfer. Proc Natl Acad Sci U S A 84:2160–2164
32. Cai Y, Wu MH, Ludeman SM, Grdina DJ, Dolan ME (1999) Role of O6-alkylguanine-DNA alkyltransferase in protecting against cyclophosphamide-induced toxicity and mutagenicity. Cancer Res 59:3059–3063
33. Cai Y, Ludeman SM, Wilson LR, Chung AB, Dolan ME (2001) Effect of O6-Benzylguanine on nitrogen mustard-induced toxicity, apoptosis, and mutagenicity in Chinese hamster ovary cells. Mol Cancer Ther 1:21–28
34. Murray D, Meyn RE (1986) Cell cycle-dependent cytotoxicity of alkylating agents: determination of nitrogen mustard-induced DNA cross-links and their repair in Chinese hamster ovary cells synchronized by centrifugal elutriation. Cancer Res 46:2324–2329
35. Schilsky RL, Dolan ME, Bertucci D, Ewesuedo RB, Vogelzang NJ, Mani S, Wilson LR, Ratain MJ (2000) Phase I clinical and pharmacological study of O6-benzylguanine followed by carmustine in patients with advanced cancer. Clin Cancer Res 6:3025–3031
36. Schwartz PS, Waxman DJ (2001) Cyclophosphamide induces caspase 9-dependent apoptosis in 9L tumor cells. Mol Pharmacol 60:1268–1279
37. Ricotti L, Barzanti F, Tesei A, Amadori D, Gasperi-Campani A, Frassineti GL, Zoli W (2000) Combined 4-hydroxy-ifosfamide and vinorelbine treatment in established and primary human breast cell cultures. Ann Oncol 11:587–594
38. Latz D, Schulze T, Manegold C, Schraube P, Flentje M, Weber KJ (1998) Combined effects of ionizing radiation and 4-hydroperoxyfosfamide in vitro. Radiother Oncol 46:279–283
39. Kuraoka I, Kobertz WR, Ariza RR, Biggerstaff M, Essigmann JM, Wood RD (2000) Repair of an interstrand DNA cross-link initiated by ERCC1-XPF repair/recombination nuclease. J Biol Chem 275:26632–26636
40. Lindahl T, Wood RD (1999) Quality control by DNA repair. Science 286:1897–1905
41. Arris CE, Boyle FT, Calvert AH, Curtin NJ, Endicott JA, Garman EF, Gibson AE, Golding BT, Grant S, Griffin RJ, Jewsbury P, Johnson LN, Lawrie AM, Newell DR, Noble ME, Sausville EA, Schultz R, Yu W (2000) Identification of novel purine and pyrimidine cyclin-dependent kinase inhibitors with distinct molecular interactions and tumor cell growth inhibition profiles. J Med Chem 43:2797–2804
42. Davies TG, Bentley J, Arris CE, Boyle FT, Curtin NJ, Endicott JA, Gibson AE, Golding BT, Griffin RJ, Hardcastle IR, Jewsbury P, Johnson LN, Mesguiche V, Newell DR, Noble ME, Tucker JA, Wang L, Whitfield HJ (2002) Structure-based design of a potent purine-based cyclin-dependent kinase inhibitor. Nat Struct Biol 9:745–749

43. Gibson AE, Arris CE, Bentley J, Boyle FT, Curtin NJ, Davies TG, Endicott JA, Golding BT, Grant S, Griffin RJ, Jewsbury P, Johnson LN, Mesguiche V, Newell DR, Noble ME, Tucker JA, Whitfield HJ (2002) Probing the ATP ribose-binding domain of cyclin-dependent kinases 1 and 2 with O(6)-substituted guanine derivatives. J Med Chem 45:3381–3393
44. Ludeman SM (1999) The chemistry of the metabolites of cyclophosphamide. Curr Pharm Des 5:627–643
45. Flowers JL, Ludeman SM, Gamcsik MP, Colvin OM, Shao KL, Boal JH, Springer JB, Adams DJ (2000) Evidence for a role of chloroethylaziridine in the cytotoxicity of cyclophosphamide. Cancer Chemother Pharmacol 45:335–344